

# What did we learn from gamma-ray burst 080319B ?

P. Kumar<sup>1</sup> and A. Panaitescu<sup>2</sup>

<sup>1</sup> *Department of Astronomy, University of Texas, Austin, TX 78712, USA*

<sup>2</sup> *Space Science and Applications, Los Alamos National Laboratory, Los Alamos, NM 87545, USA*

## ABSTRACT

The optical and gamma-ray observations of GRB 080319B allow us to provide a broad-brush picture for this remarkable burst. The data indicate that the prompt optical and gamma-ray photons were possibly produced at the same location but by different radiation processes: synchrotron and synchrotron self-Compton, respectively (but we note that this interpretation of the gamma-ray data faces some difficulties). We find that the burst prompt optical emission was produced at a distance of  $10^{16.3}$  cm by an ultra-relativistic source moving at Lorentz factor of  $\sim 500$ . A straightforward inference is that about 10 times more energy must have been radiated at tens of GeV than that released at 1 MeV. Assuming that the GRB outflow was baryonic and that the gamma-ray source was shock-heated plasma, the collimation-corrected kinetic energy of the jet powering GRB 080319B was larger than  $10^{52.3}$  erg. The decay of the early afterglow optical emission (up to 1 ks) is too fast to be attributed to the reverse shock crossing the GRB ejecta but is consistent with the expectations for the “large-angle” emission released during the burst. The pure power-law decay of the optical afterglow flux from 1 ks to 10 day is most naturally identified with the (synchrotron) emission from the shock propagating into a wind-like medium. However, the X-ray afterglow requires a departure from the standard blast-wave model.

**Key words:** radiation mechanisms: non-thermal - shock waves - gamma-rays: bursts

## 1 INTRODUCTION

Our understanding of gamma-ray bursts (GRBs) has improved tremendously in the last ten years. Observations have firmly established that GRBs and their afterglows arise from highly relativistic (Taylor et al 2004), collimated outflows (Frail et al 2001, Panaitescu & Kumar 2002). At least a few long-duration GRBs are associated with the collapse of massive stars (Galama et al 1998, Della Valle et al 2003, Hjorth et al 2003, Malesani et al 2004), but less than a few percent of supernovae of Type Ib/c give rise to GRBs (Soderberg et al 2004). A fraction of short-duration GRBs are associated with old stellar populations (Nakar 2007).

Among the fundamental questions that remain unanswered is the generation of  $\gamma$ -rays and the composition of the relativistic jet (baryonic,  $e^\pm$  and/or magnetic). The simultaneous monitoring of the optical and  $\gamma$ -ray emissions of GRB 080319B can provide insight into the mechanism for  $\gamma$ -ray generation, as described in the next section.

Studies of the multiwavelength prompt emission are still incipient because of the rarity of a good temporal coverage of the optical counterpart. So far, the prompt optical emission was observed (*i*) to be decoupled from that at  $\gamma$ -rays (GRB 990123 – Akerlof et al 1999), (*ii*) to contain a fluctuating component that tracks the burst and a smooth one peaking after the burst (GRB 050820A – Vestrand et al 2006), or (*iii*) to fluctuate in phase with the burst (GRB 041219A – Vestrand et al 2005). GRB 080319B is of the last type.

## 2 PROMPT RADIATION

### 2.1 Synchrotron self-Compton model

GRB 080319B was the brightest burst detected by Swift. It was also seen by the Konus satellite, which measured its fluence in the 20 keV – 7 MeV band,  $\Phi_\gamma = (5.7 \pm 0.1) \times 10^{-4}$  erg cm<sup>-2</sup>, corresponding to an isotropic energy release of  $E_\gamma = 1.3 \times 10^{54}$  erg (Golenetskii et al 2008), for the burst redshift  $z = 0.937$  (Vreeswijk et al 2008, Cucchiara & Fox 2008). The time-averaged spectrum during the burst peaked at 650 keV. The Konus spectrum was  $F_\nu \propto \nu^{0.18 \pm 0.01}$  below its peak at 650 keV and  $F_\nu \propto \nu^{-2.87 \pm 0.44}$  above it.

The peak optical flux during the burst was  $V = 5.4$  mag (Karpov et al 2008), detectable with unaided eye for about 30 s under appropriate conditions. The optical and the gamma-ray light-curves of GRB 080319B shown in Figure 1 are mildly correlated, suggesting that both radiations originated from the same source. The optical-gamma-ray correlation function for the entire prompt emission has a maximum at lags between 0s and 5s, that being mostly the result of the contemporaneous rise at 0-18 s and fall at 43-60 s. For the middle part of prompt emission, the optical-gamma-ray correlation function still has a peak at lags between -1s to 3s, but is less prominent.

The time-lag between the (GRB) emission produced in (say) internal shocks and the (optical) emission released by the blast-wave caused by the ejecta interaction with the

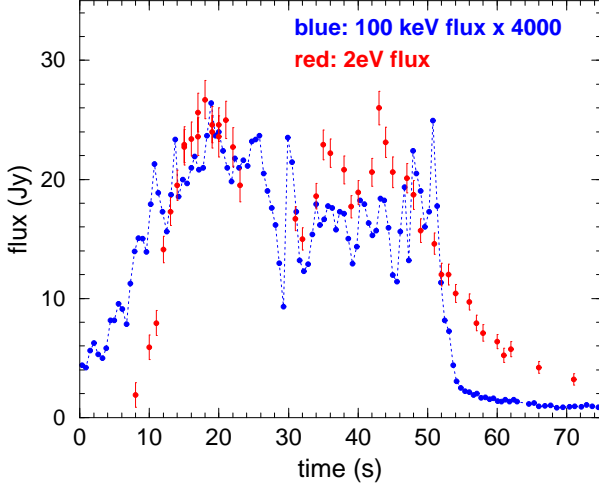


**Figure 1.** Prompt gamma-ray and optical light-curves of GRB 080319B. The high energy flux was multiplied by 4000 to allow comparison with the much larger optical flux. The burst gamma-ray emission was monitored by the Swift BAT instrument at 15–150 keV (data shown here are courtesy of T. Sakamoto and S. Barthelmy). The optical counterpart emission was measured by the Tortora collaboration (Karpov et al 2008). The finer time-sampling of the burst light-curve reveals more variability than can be seen in the optical emission, still the two light-curves appear correlated: the three optical peaks at 18, 35, and 43 s correspond to peaks of the GRB emission.

ambient medium can be arbitrarily small, thus the optical and  $\gamma$ -ray fluctuations could be correlated (as seen for GRB 080319B) even though they arise from different sources. However, the short duration  $\delta t$  of the optical pulses (with  $0.2 \lesssim \delta t/t \lesssim 0.5$ ) and the lack of an increasing optical pulse duration throughout the burst (instead, a decrease is apparent), as expected for an increasing source radius, argue against an origin of the optical counterpart in the external shock (either the reverse-shock crossing the ejecta or the forward-shock propagating in the circumburst medium). This makes it more likely that the two prompt emissions are, in fact, arising from same source.

The extrapolation of the gamma-ray spectrum (which peaks at 650 keV and has a peak flux of about 7 mJy) to the optical band under-predicts the observed optical counterpart flux (which is around 20 Jy) by almost 4 orders of magnitude. This indicates that, although from same source, the optical and gamma-ray radiation processes are different. A natural possibility is that optical photons were generated via the synchrotron emission and gamma-rays via inverse-Compton scatterings of that synchrotron emission (i.e. *synchrotron self-Compton* mechanism).

The peak energy of the synchrotron spectrum ( $\nu_i$ ) should be below optical, to account for the optical spectrum of  $F_\nu \propto \nu^{-2/3}$  (Woźniak et al 2008): measured by Raptor after 80 s. We parameterize the synchrotron peak photon energy as  $\nu_{io}$  eV ( $\nu_{io} \lesssim 1$ ), above which the optical counterpart spectrum has a spectral index  $\beta_o$  (i.e.  $F_\nu \propto \nu^{-\beta_o}$ ). The measured peak energy of the  $\gamma$ -ray burst spectrum, which is the inverse-Compton scattering of synchrotron photons, implies that the radiating electrons have a random Lorentz factor  $\gamma_e = (650 \text{ keV} / 5 \nu_{io} \text{ eV})^{1/2} \sim 360 \nu_{io}^{-1/2}$ ,

where the factor 5 accounts for the scattering by a population of electrons with a power-law distribution with energy above  $\gamma_e$ . The second inverse-Compton scattering component should peak at  $5\gamma_e^2 * 650 \text{ keV} \sim 400 \nu_{io}^{-1} \text{ GeV}$  and its fluence should be larger than that of the gamma-rays by a factor equal to the gamma-ray to optical fluence ratio:  $Y_1 = (650 \text{ keV} * 7 \text{ mJy}) / (2 \text{ eV} * 20 \text{ mJy} * \nu_{io}^{1-\beta_o}) \sim 100$  (this ratio is the “Compton parameter”). Hence, the fluence of the  $\sim 400 \text{ GeV}$  emission accompanying GRB 080319B should have been  $\Phi_{GeV} = Y_1 \Phi_\gamma \sim 0.05 \text{ erg cm}^{-2}$ ; the GLAST/LAT instrument would collect thousands photons at 0.1–100 GeV during a burst as bright as GRB 080319B.

For the isotropic-equivalent gamma-ray output of GRB 080319B of  $E_\gamma \sim 10^{54} \text{ erg}$ , the Compton parameter above implies a GeV output of  $E_{GeV} \simeq Y_1 E_\gamma \sim 10^{56} \text{ erg}$ . The energy release is smaller if the second inverse-Compton scattering is in the Klein-Nishina regime. The total energy release is reduced further by a few orders of magnitude if the fireball is tightly collimated (i.e. the explosion energy is released in a narrow jet). These reduction factors are estimated below.

As the peak of the synchrotron spectrum is at  $\nu_i = 10^{6.6} (z+1)^{-1} B \Gamma \gamma_e \text{ Hz}$ , where  $B$  is the source’s magnetic field and  $\Gamma$  its bulk Lorentz factor, the inferred random Lorentz factor  $\gamma_e$  of the radiating electrons and the peak frequency of the synchrotron spectrum imply that  $B \Gamma \sim 10^3 \nu_{io}^2 \text{ Gauss}$ . For a burst redshift  $z = 0.94$ , the peak flux of the synchrotron emission is  $F_p = 10^{-56.2} \Gamma B N_e \text{ Jy}$ , where  $N_e$  is the number of radiating electrons, thus observed synchrotron optical peak flux of  $\sim 20 \text{ Jy}$  requires that  $N_e \sim 10^{54.5} \nu_{io}^{-\beta_o-2}$ . The optical thickness of the source to Thomson scattering ( $\tau_e$ ) is the ratio of the inverse-Compton peak flux (at 650 keV) and the synchrotron peak flux:  $\tau_e \sim 10^{-3.5} \nu_{io}^{\beta_o}$ . Using that  $\tau_e = \sigma_{Th} N_e / (4\pi R_\gamma^2)$ , where  $\sigma_{Th}$  is the electron cross-section for Thomson scattering, it follows that the GRB source radius is  $R_\gamma \sim 10^{16.3} \nu_{io}^{-\beta_o-1} \text{ cm}$ . This distance is a factor  $\sim 100$  larger than that expected (eg. Piran 2005) for internal shocks.

The very steep decline of gamma-ray and optical flux at the end of the burst suggests that the source turned-off quickly. The flux decline cannot be faster than the limit provided by the photons emitted from source regions outside the  $\Gamma^{-1}$  opening area moving toward the observer. This “large-angle” emission arising from the fluid moving at an angle larger than  $\Gamma^{-1}$  yields a flux decay  $F_\gamma \propto t^{-\beta_\gamma-2}$  (Fenimore & Sumner 1997, Kumar & Panaitescu 2000). Since the burst emission has  $\beta_\gamma \sim 0$  in the 15–150 keV BAT window (Cumings et al 2008), the large-angle emission should decay as  $F_\gamma \propto t^{-2}$ , i.e. much slower than the fall-off displayed by the burst emission at 50–55 s (Figure 2). The observed decay of the burst tail can be reconciled with the upper limit set by the large-angle emission if the last GRB pulse is timed not since the burst trigger (e.g. Fan & Wei 2005) but since a reference time  $t_0 = 48$  after it, when the relativistic ejecta producing the last GRB pulse must have been released.

This means that the timescale of the GRB pulse decay is  $\delta t \sim 3 \text{ s}$ . Taking into account that  $\delta t = (z+1) R_\gamma / (2c\Gamma^2)$ , the inferred burst radius implies a source Lorentz factor  $\Gamma \sim 500 \nu_{io}^{-(\beta_o+1)/2}$ . Then, from  $B \Gamma \sim 10^3 \nu_{io}^2 \text{ G}$ , we find that the magnetic field in the GRB source is  $B \sim 2 \nu_{io}^{(\beta_o+5)/2} \text{ G}$ .

The GRB source radius can be used to constrain the location of the synchrotron peak frequency ( $\nu_{io}$ ). The lack of a progressive lengthening of the burst pulse throughout

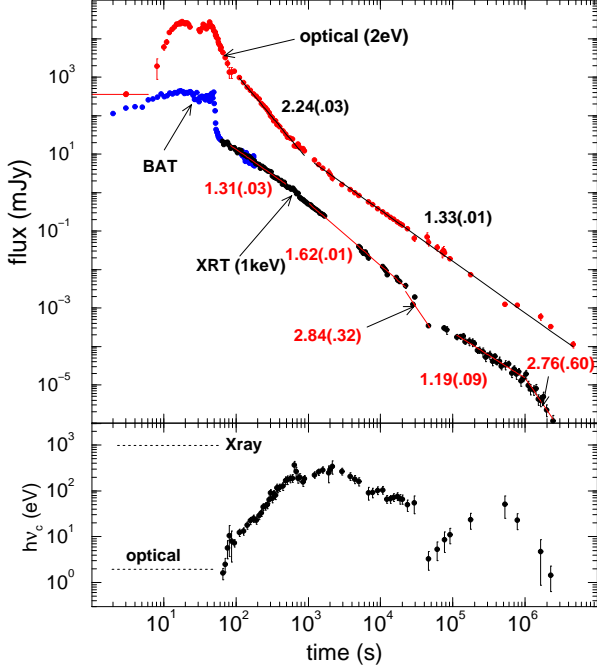


**Figure 2.** *Top panel:* prompt and afterglow X-ray and optical light-curves of GRB 080319B. The BAT measurements of the prompt 15–150 keV emission have been shifted vertically to match the XRT flux at 65–180 s. The XRT 0.3–10 keV afterglow measurements are from the Evans et al (2007) site and the 1 keV flux was calculated using the spectrum  $F_\nu \propto \nu^{-0.92 \pm 0.07}$  reported by Racusin et al (2008). Optical measurements are from Bloom et al (2008) and have been supplemented with the measurements after 1 day reported in GCN 7535 (D. Perley et al), 7569 (N. Tanvir et al), 7621 (N. Tanvir et al), and 7710 (A. Levan et al). Power-law fits to segments of each light-curve are shown. Numbers indicate the index (and uncertainty) of the power-law decay exponent  $\alpha$  defined by  $F_{o,x} \propto t^{-\alpha}$ . *Bottom panel:* evolution of the cooling break frequency  $\nu_c$  required to accommodate the afterglow optical and X-ray fluxes with the same spectral component. This frequency is calculated from the slope of the X-ray continuum, taking into account that below  $\nu_c$  the slope of the synchrotron spectrum is smaller by 1/2 than above it. Extinction of the optical emission by dust in the host galaxy is negligible (Bloom et al 2008).

the burst indicates that the GRB source is not decelerating. The radius at which the ejecta are decelerated by their interaction with the wind expelled by the Wolf-Rayet progenitor is  $R_d \sim 10^{17} \nu_{io}^{\beta_o+1}$  cm, provided that the kinetic energy of the ejecta is similar to the radiation output. The condition  $R_\gamma < R_d$  leads to  $\nu_{io} \gtrsim 0.5$ . At the same time, at the end of the burst, the peak of the synchrotron spectrum cannot be well above 1 eV (i.e.  $\nu_{io} \lesssim 3$ ) because that would bring the synchrotron self-absorption frequency above the optical and yield a constant optical flux from the large-angle emission, which is inconsistent with observations of a decaying optical flux after the burst end. Thus, to a good approximation,  $\nu_{io} \sim 1$ , implying that the time averaged optical spectrum during the burst should have been rather flat.

For the inferred  $\gamma_e$  and  $\Gamma$ , the second inverse-Compton scattering occurs just above the Klein-Nishina limit, where the electron scattering cross-section is  $\sim 0.4\sigma_{Th}$ . Therefore the twice-scattered photon takes all the electron energy, the

peak energy of the 2nd inverse-Compton component being at  $\Gamma\gamma_e m_e c^2 (z+1)^{-1} \sim 50$  GeV and the Compton parameter for the 2nd scattering being  $Y_2 = 0.4 \tau_e \gamma_e m_e c^2 / [650 (z+1) \Gamma^{-1} \text{ keV}] \sim 10$  (i.e. 10 times smaller than for the first scattering). Thus, the isotropic-equivalent total radiation output of GRB 080319B was  $E_{rad} = Y_2 E_\gamma \sim 10^{55}$  erg.

From the inferred  $B$ ,  $\Gamma$ , and  $Y$  (for first and second scattering), it can be shown that the cooling electron Lorentz factor  $\gamma_c = 6\pi m_e c^2 \Gamma / (Y_1 Y_2 R_\gamma B^2) \sim 150$ , thus  $\gamma_c < \gamma_e$  and the GRB electrons are fast-cooling (Sari, Piran & Narayan 1998). This has two consequences. First, since the GRB spectrum does not exhibit a  $F_\nu \propto \nu^{-1/2}$  spectrum below its peak, as expected for radiatively-cooling electrons, a re-acceleration process must be active during the burst. Second, at the end of burst, when electrons are no longer accelerated, the peak energy of the inverse-Compton spectrum falls fast below the BAT window and the emission from the  $\Gamma^{-1}$  region moving toward the observer decreases on a timescale shorter than  $\delta t$ , allowing the large-angle emission to become dominant (i.e. initial assumption that the GRB tail is the large-angle emission is self-consistent).

If the GRB ejecta were baryonic with one proton per electron, then the energy stored in protons were larger by that of electrons by a factor of at least  $m_p/(\gamma_e m_e) \sim 5$ , implying that the total GRB outflow energy is at least 5 times larger than the radiated energy. Thus the total isotropic-equivalent energy release in this GRB explosion must have been  $E_k \gtrsim 5 E_{rad} \sim 10^{55.7}$  erg.

## 2.2 Limitations/drawbacks of the model

Although the synchrotron self-Compton model is a *natural* interpretation of the optical and gamma-ray prompt emission from GRB 080319B, it suffers from a few, possibly serious, problems.

One of the problems is the incompatibility between the observed and expected gamma-ray spectrum. In the synchrotron-self Compton model, the synchrotron (optical) and inverse-Compton (gamma-rays) spectra are closely related. The model parameters derived above lead to an up-scattered self-absorbed photon energy of  $\sim 100$  keV, below which the inverse-Compton spectrum should be  $F_\nu \propto \nu$  (Panaitescu & Mészáros 2000). In contrast, Golenetskii et al (2008) measure for GRB 080319B a softer  $F_\nu \propto \nu^{0.2}$  gamma-ray spectrum down to 20 keV. A similar inconsistency between the self-Compton model and gamma-ray observations is encountered for GRB 990123, which we (Panaitescu & Kumar 2007) suggested that could be explained if the magnetic field decays (Rossi & Rees 2003) on a length-scale much larger than the plasma skin depth.

Furthermore, in the large-angle emission interpretation of the early, steep optical decay (§3.1), the optical spectral slope  $\beta_o = 2/3$  measured by Woźniak et al (2008) during that decay is just the slope above the peak of the synchrotron spectrum of the prompt emission. However, that is inconsistent with the spectral slope of the inverse-Compton emission above the GRB spectral peak, which Golenetskii et al (2008) report to be much softer,  $\beta_\gamma = 2.9 \pm 0.4$ . The possible solution to this problem is that the early optical afterglow emission of GRB 080319B, which we identify with the large-angle emission released during the burst, is dominated by that from a single pulse whose spectrum is harder above its

spectral peak than that of the burst-averaged gamma-ray spectrum. Taking into account that the decay of the large-angle emission from a pulse lasting  $\delta t$ , peaking at  $t_p$ , and of peak flux  $F_p$ , is  $F_{lae}(t) = F_p[(t - t_p)/\delta t]^{-2-\beta_o}$ , it seems plausible that the large-angle emission is dominated by the pulse with the hardest spectral slope  $\beta_o$ .

Another potential problem for the synchrotron self-Compton interpretation of GRB 080319B's prompt emission is that the gamma-ray light-curve exhibits a higher variability than the optical counterpart, as one would expect the inverse-Compton gamma-ray emission to have less fluctuations than the synchrotron seed photon field.

We note that the rise of the optical counterpart emission lagging that of the gamma-rays could be due to the optical band being below the synchrotron self-absorption frequency at early times. In this case, the adiabatic cooling of ejecta electrons leads to a steep rise ( $t^3$ ), consistent with that displayed by the optical emission at 8–15 s. At the other end, the optical counterpart emission turned-off before the gamma-rays. That the last three GRB pulses are not accompanied by optical emission may be due to that their synchrotron spectrum peaked sufficiently below the optical.

### 3 AFTERGLOW EMISSION

#### 3.1 Steep, early optical decay ( $t < 1$ ks)

After the burst, the optical emission has a spectral slope  $\beta_o \simeq 0.65$  and displays a steep decay,  $F_o \propto t^{-2.8}$  up to 1 ks, as shown in Figure 3, where the contribution of the power-law decaying emission after 1 ks,  $F_o \propto t^{-1.3}$ , was subtracted from the earlier optical flux. Assuming that the burst ejecta is in pressure equilibrium with the ambient medium shocked by the forward shock, whose structure is described by the Blandford-McKee solution, we find that the steepest decay for the synchrotron emission from the ejecta electrons, after they have been energized by the reverse-shock (i.e. as they cool adiabatically), is obtained for a wind-like medium and an ejecta shell thickness increasing as  $R/\Gamma_{rs}$ , with  $R$  the shock radius and  $\Gamma_{rs}$  its Lorentz factor. That decay,  $\alpha_{rs} = 1.47\beta_o + 0.80 = 1.75$  (see equation 55 of Panaitescu & Kumar 2004) is too slow to account for the decay measured for GRB afterglow 080319B at 100–1000 s (the results of Sari & Piran 1999 and Kobayashi & Sari 2000 for the reverse-shock emission give a steeper decay, up to  $\alpha_{rs} = 2.0$ , which is still too slow to account for the observed  $F_o \propto t^{-2.8}$ ).

Instead, the optical light-curve decline is consistent with the large-angle emission model, for which  $F_o \propto t^{-2-\beta_o}$  is expected. Therefore, we suggest that the optical afterglow emission between 50 s and 1 ks arises from the same source that produced  $\gamma$ -ray photons.

#### 3.2 Afterglow emission after 1 ks

The slower decay of the optical flux observed after 1 ks,  $F_o \propto t^{-1.33 \pm 0.01}$  (Figure 2), is most naturally attributed to the emission from the forward-shock driven into the ambient medium (e.g. Paczyński & Rhoads 1993, Mészáros & Rees 1997) by the burst ejecta overtaking the large-angle burst emission. The optical flux decay ( $F_o \propto t^{-\alpha_o}$ ) and spectral

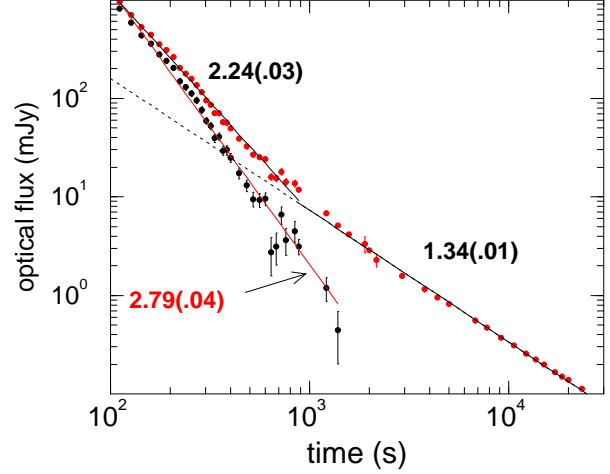


**Figure 3.** Subtraction of the extrapolation (solid black line) to earlier times of the afterglow optical emission after 1 ks reveals that the excess of optical flux before 1 ks has a decay  $F_o \propto t^{-2.8}$  (red line).

slope  $F_\nu \propto \nu^{-0.63 \pm 0.07}$  at 90 ks (Bloom et al 2008) satisfy  $\alpha_o - 1.5\beta_o = 0.39 \pm 0.10$ , which is consistent only with a circumburst medium density of  $r^{-2}$  radial structure and cooling frequency of the forward-shock synchrotron spectrum above optical (for which  $F_o \propto t^{-(3\beta_o+1)/2}$  is expected – Chevalier & Li 1999). A homogeneous circumburst medium, for which  $\alpha_o - 1.5\beta_o = 0$  or  $-0.5$  (depending on the location of the cooling break) is inconsistent with the observations at the  $4\sigma$  level.

The X-ray light-curve should exhibit the same decay as the optical if the cooling break frequency is not between optical and X-ray or, owing to a wind-like medium, a slower one with decay index  $\alpha_x = \alpha_o - 1/4$  if the cooling frequency is between these domains. The former could be the case for the early (before 1 ks) X-ray light-curve, whose decay is compatible with that seen in the optical after 1 ks, but neither expectation is satisfied by the X-ray and optical decays after 1 ks, for which  $\alpha_x = \alpha_o + 1/3$ . The same inconsistency with the standard blast-wave model expectations is also illustrated in the lower panel of Figure 2, which shows that, if the optical and X-ray afterglow emissions were attributed to the same spectral component, then the cooling break would have to exhibit a non-monotonic evolution incompatible with the blast-wave model, in general, and with the  $\nu_c \propto t^{1/2}$  evolution expected for wind medium, in particular.

The non-monotonic evolution of the cooling break shown in Figure 2 suggests a departure from the basic assumptions of the standard blast-wave model, such as a non-monotonically evolving magnetic field energy parameter (on which the cooling frequency has the strongest dependence). Alternately, the optical and X-ray afterglow emissions may have (somewhat) different origins. For instance, the optical flux, which exhibits a single power-law decay after 1 ks, could be attributed to the synchrotron emission from the forward shock, while the X-ray flux, which displays 5 power-law segments, could arise from reprocessing of the forward-shock emission by scattering off a lagged part of the relativistic outflow (Panaitescu 2008).

For GRB ejecta collimated into a jet of half-angle  $\theta_j$ , the afterglow light-curve should exhibit a steepening to a decay faster than  $t^{-1.5}$  when the jet edge becomes visible to the observer. Using the arrival time of photons emitted at angle  $\Gamma^{-1}$  and for a circumburst medium of density typical for Galactic Wolf-Rayet stars, the jet-break time is  $t_b = 200(z+1)(E_k/10^{55.7})(\theta_j/0.1)^4$  d. Since the optical light-curve of GRB 080319B afterglows does not exhibit a jet-break during the first 10 days (Figure 2), the jet opening is  $\theta_j \gtrsim 2$  deg. Therefore, the collimation-corrected kinetic energy of the GRB outflow is  $E_{jet} = E_k(\theta_j^2/4) \gtrsim 10^{52.3}$  erg.

#### 4 CONCLUSIONS

The modest correlation between the optical and gamma-ray light-curves of GRB 080319B suggests that these emissions may be from the same source. That the prompt optical flux lies well above the extrapolation of the burst spectrum to optical indicates that the two emissions arose from different radiation processes: optical emission was generated through synchrotron process and  $\gamma$ -rays were due to inverse-Compton scattering of the synchrotron photons. As shown by (Kumar & McMahon 2008), a bright optical emission accompanying  $\gamma$ -rays is a generic prediction of the synchrotron self-Compton model for GRBs. However, some features of the gamma-ray data for GRB 080319B are not accounted for by that model, as discussed in §2.2.

Synchrotron self-Compton emission may have also been observed during GRB 990123 (Panaiteescu & Kumar 2007). For the bright optical counterpart of GRB 080319B, we find that the spectrum of the synchrotron prompt emission must have peaked in the optical, while for GRB 990123 that peak was slightly above optical, which can explain (at least in part) why these optical counterparts were so bright.

Within the synchrotron self-Compton model for the prompt emission and without any assumption about the dissipation mechanism, we have shown that the  $\gamma$ -ray and optical measurements of GRB 080319B imply a source radius of  $10^{16.3}$  cm, moving at Lorentz factor 500. The energy of the 2nd inverse-Compton scattering, which should have peaked at  $\sim 50$  GeV, must have been 10 times larger than that of the 1st inverse-Compton component at sub-MeV energies. With the lower limit on the half-angle of the GRB outflow set by the lack of an afterglow optical light-curve break until 10 d, and assuming a baryonic, shock-heated  $\gamma$ -ray source, we estimate that the beaming-corrected kinetic energy of outflow powering GRB 080319B was higher than  $10^{52.3}$  erg (twice larger for a double-sided jet), which provides an important constraint for the collapsar model (MacFadyen & Woosley 1999, Woosley & Bloom 2006) for long bursts.

We find that the optical light-curve decay at 0.1–1 ks is too fast to be attributed to the external reverse-shock propagating into the GRB ejecta. Instead, the early optical decay and spectral slope are consistent with the large-angle emission released during the burst and arriving at observer later, due to the spherical curvature of the emitting surface.

The decay of the late-time ( $t \gtrsim 1$  ks) optical afterglow flux is consistent with an origin in the forward-shock energizing a wind-like circumburst medium, a homogeneous medium being "ruled out" at  $4\sigma$ . However, if the optical and X-ray afterglow fluxes arose from same mechanism, an

unusual evolution of the cooling frequency would be required, which may be indicative of evolving blast-wave microphysical parameters. Alternatively, the X-ray afterglow emission may be affected by reprocessing of the optical forward-shock photons through (bulk and, possibly, inverse-Compton) scattering by a relativistic, pair-rich outflow located behind the forward shock. In this model, the scattering outflow results from continued accretion onto the central black-hole, if such an accretion can be maintained for source-frame timescales comparable to the observer-frame duration of the X-ray afterglow.

#### ACKNOWLEDGMENTS

The authors are grateful to the referee for his comments. AP acknowledges the support of the US Department of Energy through the LANL/LDRD 20080039DR program and of NASA Swift GI grant NNG06EN001 for this work.

#### REFERENCES

- Bloom J. et al., 2008, preprint (arXiv:0803.3215)
- Chevalier R., Li, Y., 1999, ApJ, 520, L29
- Cucchiara A., Fox D., 2008, GCN 7456\*
- Cummings J. et al., 2008, GCN 7462\*
- Della Valle M. et al., 2003, A&A, 406, L33
- Evans P. et al., 2007, A&A, 469, 379
- Fan Y., Wei D., 2005, MNRAS, 364, L42
- Fenimore E., Sumner M., 1997, in "All-Sky X-ray Observations in the Next Decade", eds. M. Matsuoka and N. Kawai, Riken, Japan, p.167 (astro-ph/9705052)
- Frail D. et al., 2001, ApJ, 562, L55
- Galama T. et al., 1998, Nature, 395, 670
- Golenetskii S. et al., 2008, GCN 7482\*
- Hjorth J. et al., 2003, Nature, 423, 847
- Karpov S. et al., 2008, GCN 7558\*
- Kobayashi S., Sari R., 2000, ApJ, 542, 819
- Kumar P., Panaiteescu A., 2000, ApJ, 541, L51
- Kumar P., McMahon E., 2008, MNRAS, 384, 33
- MacFadyen A., Woosley S., 1999, ApJ, 524, 262
- Malesani D. et al., 2004, ApJ, 609, L5
- Mészáros P., Rees M., 1997, ApJ, 476, 232
- Nakar E., 2007, Physics Rep., 442, 166
- Paczynski B., Rhoads J., 1993, ApJ, 418, L5
- Panaiteescu A., Mészáros P., 2000, ApJ, 544, L17
- Panaiteescu A., Kumar P., 2002, ApJ, 571, 779
- Panaiteescu A., Kumar P., 2004, MNRAS, 353, 511
- Panaiteescu A., Kumar P., 2007, MNRAS, 376, 1065
- Panaiteescu A., 2008, MNRAS, 383, 1143
- Piran T., 2005, Rev. Mod. Phys., 76, 1143
- Racusin J. et al., 2008, GCN 7459\*
- Rossi E., Rees M., 2003, MNRAS, 339, 881
- Sari R., Piran T., Narayan R., 1998, ApJ, 497, L17
- Sari R., Piran, T., 1999, ApJ, 520, 641
- Soderberg A., Frail D., Wieringa M., 2004, ApJ 607, L13
- Taylor G., Frail D., Berger E., Kulkarni S., 2004, ApJ, 609, L1
- Vreeswijk P. et al., 2008, GCN 7444\*
- Vestrand W. et al., 2005, Nature, 435, 178
- Vestrand W. et al., 2006, Nature, 442, 172
- Woosley S., Bloom J., 2006, ARA&A, 44, 507
- Woźniak P. et al., 2008, preprint

\* GCN circulars can be found at  
[http://gcn.gsfc.nasa.gov/gcn/gcn3\\_archive.html](http://gcn.gsfc.nasa.gov/gcn/gcn3_archive.html)